Measurement of the Spatial Correlation Function of Phase Fluctuating Bose-Einstein Condensates

D. Hellweg,[1,*] L. Cacciapuoti,[1] M. Kottke,[1] T. Schulte,[1] K. Sengstock,[2] W. Ertmer,[1] and J. J. Arlt[1]

[1]*Institut für Quantenoptik, Universität Hannover, Welfengarten 1, 30167 Hannover, Germany*

[2]*Institut für Laserphysik, Universität Hamburg, Luruper Chaussee 149, 22761 Hamburg, Germany*

(Received 17 March 2003; published 3 July 2003)

We measure the intensity correlation function of two interfering spatially displaced copies of phase fluctuating Bose-Einstein condensates. It is shown that this corresponds to a measurement of the phase correlation properties of the initial condensate. Analogous to the method used in the stellar interferometer experiment of Hanbury Brown and Twiss, we use spatial intensity correlations to determine the phase coherence lengths of elongated condensates. We find good agreement with our prediction of the correlation function and confirm the expected coherence length.

DOI: 10.1103/PhysRevLett.91.010406 PACS numbers: 03.75.Hh, 03.75.Nt, 39.20.+q

Since the first realization of Bose-Einstein condensation in dilute atomic gases, their coherence properties have attracted considerable theoretical and experimental interest. This interest is due to the central role of the coherence properties for the theoretical description and conceptional understanding of Bose-Einstein condensates (BECs) and their use as a source of coherent matter waves in many promising applications.

Remarkable measurements demonstrated the phase coherence of three-dimensional condensates well below the BEC transition temperature T_c [1–3] and even at finite temperature [4]. However, low dimensional systems show a qualitatively different behavior. In particular, it has been predicted that one-dimensional and even very elongated, three-dimensional BECs exhibit strong spatial and temporal fluctuations of the phase while fluctuations in their density distribution are suppressed [5,6]. Thus, the coherence properties are significantly altered, resulting in a reduced coherence length which can be much smaller than the condensate length. In this case, the degenerate sample is called a quasicondensate. This regime has been the subject of recent theoretical efforts, including an extension of the Bogoliubov theory [7], a modified mean-field theory valid in all dimensions [8,9], and a calculation of the correlation functions [10]. Phase fluctuations were first observed using the formation of density modulations during ballistic expansion of a condensate [11–13]. In addition, their effect on the momentum distribution has been demonstrated using Bragg spectroscopy [14,15]. Nonequilibrium properties of these condensates have been studied using a condensate focusing technique [16].

In this Letter, we report on a direct measurement of the spatial correlation function of phase fluctuating BECs. To measure the phase correlation properties, we interfere two copies of a BEC with a spatial displacement d (Fig. 1). The measured interference pattern is determined by the phase pattern of the original condensate and a global phase difference between the two copies introduced by the interferometer. By varying the displacement d, the first-order correlation function can, in principle, be measured. However, this method is very sensitive to fluctuations in the global phase difference, and the measurement is further complicated by the statistical nature of phase fluctuations. We show that the use of intensity correlations in the interference pattern overcomes these problems and provides the desired information about the phase correlations in the initial condensate. The result of this measurement is described by the spatial second-order correlation function and yields the phase coherence length of the BEC. In many respects, our measurement is closely related to the stellar interferometer of Hanbury Brown and Twiss [17]. They measured the intensity of starlight falling onto two detectors and computed the

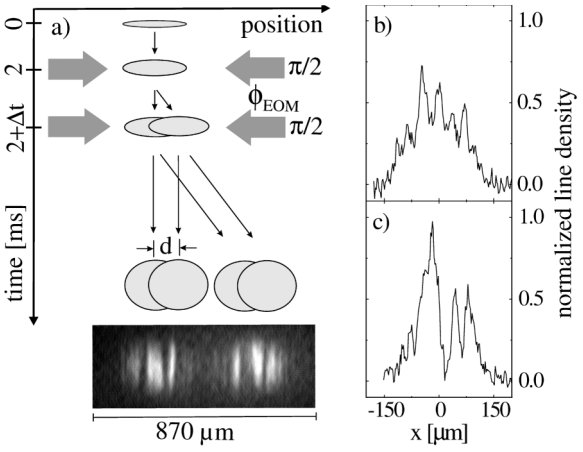

FIG. 1. (a) The interferometer is realized by two $\pi/2$ Bragg diffraction pulses. We apply the first pulse after a ballistic expansion time of 2 ms to reduce mean-field effects and atomic scattering. The spatial displacement d is determined by the time Δt between the pulses. Typical line density profiles are shown for a phase coherence length of $L_\phi \approx 25$ μm with $d = 7$ μm (b) and $d = 35$ μm (c). Only one of the two output ports is displayed.

intensity correlations electronically as a function of the detectors' distances. This measurement yields the transverse coherence length of the stellar light and allowed them to determine the stars' diameters. Unlike the Michelson stellar interferometer, which uses first-order correlations, atmospheric fluctuations do not disturb this measurement. Similarly, global phase fluctuations in the interferometer setup do not disturb our measurement.

Our experiments were performed with very elongated three-dimensional ^{87}Rb Bose-Einstein condensates in the $|F = 1, m_F = -1\rangle$ hyperfine ground state. Further details of our experimental apparatus were described previously [12]. The confining potential was provided by a cloverleaf-type magnetic trap with an axial trapping frequency of $\omega_x = 2\pi \times 3.4$ Hz and a radial frequency adjusted between $\omega_r = 2\pi \times 300$ and $\omega_r = 2\pi \times 380$ Hz. The number of condensed atoms N_0 was varied between 4×10^4 and 6×10^5. To allow the system to reach an equilibrium state, we typically waited 4 s after obtaining BEC by evaporative cooling (with rf "shielding") [18]. The interferometric scheme is shown in Fig. 1 and is based on two $\pi/2$ Bragg diffraction pulses. These pulses were produced by two counterpropagating laser beams with a frequency difference set to the two-photon resonance. They were detuned by about 3 GHz from the atomic resonance to suppress spontaneous emission. The pulse duration of 100 μs was chosen long enough to avoid higher-order diffraction and sufficiently short to avoid any sensitivity to the internal velocity distribution of the phase fluctuating BECs. After a time-of-flight of 30 to 40 ms, the two output ports spatially separate and the atoms were detected by resonant absorption imaging. We integrate the absorption images along the radial direction of the condensate and subtract the thermal background to obtain line density profiles.

Typical measured line density profiles are shown in Fig. 1. When the displacement d between the overlapping clouds is chosen smaller than the phase coherence length in the sample [Fig. 1(b)], regions with almost identical phases are brought to overlap and the resulting interference signal is rather smooth. If, however, d is larger than the phase coherence length, regions with substantially different phases overlap, resulting in an irregular but high contrast interference signal [Fig. 1(c)]. In both cases, an average over many realizations and relative phases results in the same smooth profile in the two output ports of the interferometer, revealing no information about the coherence properties. Nonetheless, Fig. 1(c) clearly contains information about the spatial coherence properties. An appropriate analysis of the correlations in the density profile yields an intensity correlation function that does not vanish in an averaging process and contains the desired information about the coherence properties.

We therefore start our analysis by calculating the spatial second-order correlation function for the case of phase fluctuating BECs. In its most general definition it is given by

$$g^{(2)}(x_1, x_2, x_3, x_4) = \frac{\langle \hat{\psi}^\dagger(x_1)\hat{\psi}^\dagger(x_2)\hat{\psi}(x_3)\hat{\psi}(x_4)\rangle_T}{\sqrt{\prod_{i=1}^4 \langle \hat{\psi}^\dagger(x_i)\hat{\psi}(x_i)\rangle_T}}, \quad (1)$$

where $\langle \ldots \rangle_T$ denotes an average over an ensemble at thermal equilibrium at temperature T. It contains the spatial intensity correlation function $g^{(2)}(x_1, x_2) = g^{(2)}(x_1, x_2, x_2, x_1)$ as a special case. For 3D condensates with repulsive interactions in elongated trapping potentials, density fluctuations are suppressed by the mean-field potential [6,13,14]. Therefore the total field operator of the condensed atoms can be written as $\hat{\psi}(x) = \sqrt{n_0(x)}\exp[i\hat{\phi}(x)]$, where $\hat{\phi}(x)$ is the operator of the phase [6] and $n_0(x)$ is the density in the Thomas-Fermi approximation. For this field operator, one can show that all higher-order correlation functions can be expressed as products of the first-order correlation function [19]. Using the explicit expression of the phase operator given by Petrov *et al.* [6], we obtain the second-order correlation function:

$$g^{(2)}(x_1, x_2, x_3, x_4) = \exp\left[-\frac{1}{2l_\phi} f^{(2)}(x_1, x_2, x_3, x_4)\right], \quad (2)$$

with

$$f^{(2)}(x_1, x_2, x_3, x_4) = \frac{1}{8}\sum_j \frac{(j+2)(2j+3)}{j(j+3)(j+1)}\left[P_j^{(1,1)}\left(\frac{x_1}{L}\right) + P_j^{(1,1)}\left(\frac{x_2}{L}\right) - P_j^{(1,1)}\left(\frac{x_3}{L}\right) - P_j^{(1,1)}\left(\frac{x_4}{L}\right)\right]^2, \quad (3)$$

where $P_j^{(1,1)}$ are Jacobi polynomials, j is a positive integer, $2L$ is the condensate length, and

$$l_\phi = \frac{L_\phi}{L} = \frac{15N_0(\hbar\omega_x)^2}{32\mu k_B T} \quad (4)$$

is the phase coherence length in the condensate center (in units of L). Here μ denotes the chemical potential and k_B the Boltzmann constant. The function $f^{(2)}$ is shown in Fig. 2 and contains the functional form of phase fluctuations in elongated condensates. All experimental parameters are contained in the phase coherence length l_ϕ.

Let us demonstrate how the interferometric sequence described above can be used to measure $g^{(2)}$. In each output port of the interferometer, the superposition of two ballistically expanded spatially displaced copies of the original wave function is produced. The field operator of the atoms in one output port can be expressed as

$$\hat{\psi}_f(x, d) = \tfrac{1}{2}[\sqrt{n(x - d/2)}e^{i\hat{\phi}^+(x-d/2)} + \sqrt{n(x + d/2)}e^{i\hat{\phi}^-(x+d/2)}e^{i\phi_{\rm rel}}], \quad (5)$$

with $\hat{\phi}^\pm(x) = \hat{\phi}(x) \pm \beta x + \alpha x^2$ [20]. The linear term results from the mean-field repulsion between the copies

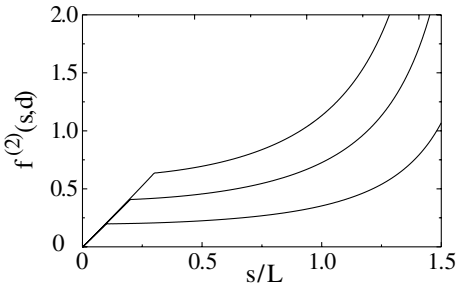

FIG. 2. Numerical computation of the function $f^{(2)}(s,d) \equiv f^{(2)}(\frac{-s-d}{2}, \frac{s+d}{2}, \frac{s-d}{2}, \frac{-s+d}{2})$ for three different d. From top to bottom: $d/L = 0.3, 0.2, 0.1$. The particular choice of positions corresponds to the experimentally relevant case.

of the condensate [21] and the quadratic term originates from the self-similar expansion [22,23]. The self-similar expanded density distribution $n(x)$ differs only slightly from the initial distribution because the increase of axial size during expansion is small for very elongated condensates (about 1% for our experimental conditions). The relative global phase between the two overlapping clouds $\phi_{\mathrm{rel}} = \delta_{12}\Delta t + \delta\phi_{\mathrm{eff}}$ is determined by the Bragg diffraction process, where $\delta\phi_{\mathrm{eff}}$ is the change in the relative phase of the Bragg beams between the two pulses and δ_{12} is the detuning from the two-photon resonance. In our experiment, $\delta\phi_{\mathrm{eff}}$ can be controlled by using an electro-optical modulator [24], δ_{12} depends on the frequency difference of the Bragg beams and the axial release velocity of the condensate. Note that even a small change in the release velocity of 0.033 μm/ms leads to a phase change of $\pi/2$ for a time $\Delta t = 3$ ms between the Bragg pulses. The insensitivity to such randomly varying global phases is a major advantage of the intensity correlation method.

In analogy to the definition of the correlation coefficient, we define a normalized intensity correlation function

$$\gamma_f^{(2)}(x_1, x_2, d) = \frac{\langle(\hat{I}_1 - \langle\hat{I}_1\rangle)(\hat{I}_2 - \langle\hat{I}_2\rangle)\rangle}{\sqrt{\langle(\hat{I}_1 - \langle\hat{I}_1\rangle)^2\rangle}\sqrt{\langle(\hat{I}_2 - \langle\hat{I}_2\rangle)^2\rangle}}, \quad (6)$$

with the intensity operator $\hat{I}_{1,2} = \hat{\psi}_f^\dagger(x_{1,2}, d)\hat{\psi}_f(x_{1,2}, d)$. Here the averages are taken over an ensemble in thermal equilibrium and over all relative phases. The possible values of $\gamma_f^{(2)}$ range between $+1$ (perfect correlation) and -1 (perfect anticorrelation); if $\hat{I}_1$ and $\hat{I}_2$ are uncorrelated $\gamma_f^{(2)} = 0$. By substituting Eq. (5) into Eq. (6), we obtain

$$\gamma_f^{(2)}(x_1, x_2, d) = \cos[2(x_1 - x_2)(\alpha d - \beta)] \times \exp\left[-\frac{1}{2l_\phi} f^{(2)}\left(x_1 - \frac{d}{2}, x_2 + \frac{d}{2}, x_2 - \frac{d}{2}, x_1 + \frac{d}{2}\right)\right]. \quad (7)$$

The normalized intensity correlation function is the product of two contributions. A cosine resulting from the self-similar expansion and mean-field repulsion and an exponentially decaying term containing the influence of the phase fluctuations. The decay constant of this function is the phase coherence length. Comparison with Eq. (2) shows that a measurement of $\gamma_f^{(2)}$ is equivalent to a measurement of the second-order correlation function of the trapped condensate.

The measurement of $\gamma_f^{(2)}$ is performed in the following way: For a given trap configuration, evaporative cooling ramp, and fixed displacement d, a series of measurements is recorded by scanning the relative phase of the Bragg beams with the electro-optical modulator in small steps between 0 and 2π. This ensures that the global phase ϕ_{rel} contains all values with equal probability. We experimentally determine $\gamma_f^{(2)}$ analogous to Eq. (6). The ensemble averages $\langle\hat{I}(x)\rangle$ are obtained by averaging all interference patterns $I(x)$ recorded in a series. Then the quantity $I(x) - \langle\hat{I}(x)\rangle$ can be determined for each realization. The average of these values according to Eq. (6) yields $\gamma_f^{(2)}$. To simplify the analysis, we evaluate $\gamma_f^{(2)}$ at symmetric positions around the center of the interference pattern such that $x_1 = -x_2 = s/2$. Then $\gamma_f^{(2)}(s, d) = \gamma_f^{(2)}(-s/2, s/2, d)$ can be expressed as a function of s for a given displacement d. Typical results are shown in Fig. 3, clearly displaying the functional form of a damped cosine.

To extract quantitative results, we fit the measured function with the theoretical function given in Eq. (7). The fit contains only l_ϕ and the frequency of the cosine as free parameters. Figure 3 compares measured correlation functions with the corresponding fits, confirming the excellent agreement with the expected functional form. Although the phase coherence length also depends on the trapping potential and the temperature, the data sets shown in Fig. 3 differ mainly due to the number of condensed atoms, which was set to 4.4×10^4 (●), 2.9×10^5 (+), and 5.0×10^5 (□). Except for the smallest atom number, a minimum is clearly visible and unambiguously defines the frequency of the cosine [25]. The damping of this oscillation yields the phase coherence length. As expected [see Eq. (4)], the damping is stronger for small N_0. In the case of the smallest N_0, no oscillation is visible, indicating a significant decrease of the phase coherence length.

We have performed such measurements for a large variety of atom numbers and temperatures. The good agreement between the measured phase coherence length obtained from the fit and the theoretically predicted result is shown in Fig. 4. By varying the displacement d, we have confirmed that the measured phase coherence lengths are independent of this parameter. In all cases, the phase coherence length was much smaller than the condensate length, which ranged from 280 up to 420 μm, i.e., our measurements were performed in the quasicondensate regime.

Thus far we have neglected the evolution of the phase fluctuations during ballistic expansion. This evolution

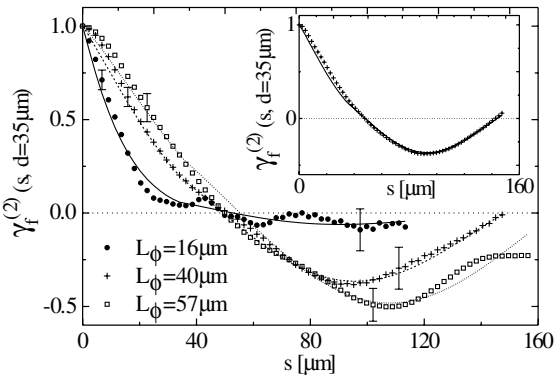

FIG. 3. Measured correlation functions (points) compared to fitted theoretical curves (lines). Each measured function is based on ≈ 25 realizations and plotted up to $s = 0.8L$. Neighboring points are not independent since they are based on a common set of experimental realizations. The error bars represent the statistical uncertainty. Inset: Numerical simulation including the phase and density evolution (points) and the analytical function Eq. (7) (line), both for the parameters of the $L_\phi = 40$ μm curve.

leads to a change of the original phase pattern and the appearance of density modulations. Using the full evolution of the wave function [19], we have calculated the expected phase change during time of flight to be less than $\pi/10$ for our parameters. To evaluate the influence of density modulations on our measurements, we have performed numerical simulations including the phase and density evolution. The inset of Fig. 3 compares a numerical result with Eq. (7). The excellent agreement demonstrates that this evolution can be neglected for our intensity correlation measurements and justifies the use of Eq. (7) to extract the phase correlation properties.

In conclusion, we have demonstrated a new interferometric method which allows us to measure the spatial correlation function of phase fluctuating BECs. First, the second-order correlation function was calculated and it was shown that this function can be measured using intensity correlations in the interference pattern. Our measurements were then compared with these results, confirming both the expected functional form of the correlation function and the phase coherence length of the sample. We have confirmed that this technique is insensitive to fluctuations of the relative global phase during the interferometric measurement sequence.

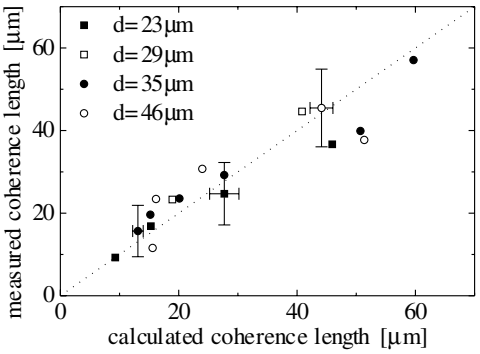

FIG. 4. Measured phase coherence length compared to the theoretically expected result given by Eq. (4). The dotted line $f(x) = x$ is a guide to the eye. The error bars indicate statistical errors. Systematic uncertainties are 26% and 15% for the calculated and measured L_ϕ, respectively.

We thank L. Santos for valuable calculations of the expansion dynamics. This work is supported by the *Deutsche Forschungsgemeinschaft* within the SFB 407.

*Electronic address: hellweg@iqo.uni-hannover.de

[1] M. R. Andrews *et al.*, Science **275**, 637 (1997).
[2] E. W. Hagley *et al.*, Phys. Rev. Lett. **83**, 3112 (1999).
[3] J. Stenger *et al.*, Phys. Rev. Lett. **82**, 4569 (1999).
[4] I. Bloch, T. W. Hänsch, and T. Esslinger, Nature (London) **403**, 166 (2000).
[5] D. S. Petrov, G. V. Shlyapnikov, and J. T. M. Walraven, Phys. Rev. Lett. **85**, 3745 (2000), and references therein.
[6] D. S. Petrov, G. V. Shlyapnikov, and J. T. M. Walraven, Phys. Rev. Lett. **87**, 050404 (2001).
[7] C. Mora and Y. Castin, Phys. Rev. A **67**, 053615 (2003).
[8] J. O. Andersen, U. Al Khawaja, and H. T. C. Stoof, Phys. Rev. Lett. **88**, 070407 (2002).
[9] U. Al Khawaja, J. O. Andersen, N. P. Proukakis, and H. T. C. Stoof, Phys. Rev. A **66**, 013615 (2002).
[10] D. L. Luxat and A. Griffin, Phys. Rev. A **67**, 043603 (2003).
[11] S. Dettmer *et al.*, Phys. Rev. Lett. **87**, 160406 (2001).
[12] D. Hellweg *et al.*, Appl. Phys. B **73**, 781 (2001).
[13] H. Kreutzmann *et al.*, Appl. Phys. B **76**, 165 (2003).
[14] S. Richard *et al.*, Phys. Rev. Lett. **91**, 010405 (2003)
[15] F. Gerbier *et al.*, Phys. Rev. A **67**, 051602 (2003).
[16] I. Shvarchuck *et al.*, Phys. Rev. Lett. **89**, 270404 (2002).
[17] R. Hanbury Brown and R. Q. Twiss, Nature (London) **177**, 27 (1956); **178**, 1046 (1956).
[18] We then observe no quadrupole oscillations. The thermalization time of our BECs was a few 100 ms.
[19] More details will be given in L. Cacciapuoti *et al.* (to be published).
[20] The origin of the x axis has been set to the center of the two overlapping clouds.
[21] J. E. Simsarian *et al.*, Phys. Rev. Lett. **85**, 2040 (2000).
[22] Y. Castin and R. Dum, Phys. Rev. Lett. **77**, 5315 (1996).
[23] Yu. Kagan, E. L. Surkov, and G. V. Shlyapnikov, Phys. Rev. A **54**, 1753(R) (1996).
[24] Y. Torii, Y. Suzuki, M. Kozuma, T. Sugiura, and T. Kuga, Phys. Rev. A **61**, 041602(R) (2000).
[25] Note that the measured frequency of the cosine is in good agreement with the prediction of α and β.